American Journal of Pathology, Vol. 133, No. 2, November 1988

Endothelial Adaptations in Aortic Stenosis

Correlation with Flow Parameters

THOMAS ZAND, MD, JOHN J. NUNNARI, MA, ALLEN H. HOFFMAN, PhD,* BRIAN J. SAVILONIS, PhD,* BRUCE MACWILLIAMS, MS,* GUIDO MAJNO, MD, and ISABELLE JORIS, PhD

From the Department of Pathology, University of Massachusetts Medical School, and Worcester Polytechnic Institute, Department of Mechanical Engineering, Worcester, Massachusetts*

A 69 ± 5% stenosis was produced in the rat aorta, with the purpose of correlating endothelial changes with local flow patterns and with levels of shear stress; the hydrodynamic data were obtained from a scaled-up model of the stenosed aorta. In the throat of the stenosis, where shear stress values were 15–25 times normal, the endothelium was stripped off within 1 hour. It regenerated at half the rate of controls but modulated into a cell type that could withstand the increased shear stress. Adaptations included changes in cell orientation, number, length, width, thickness, stress fibers, and anchoring structures, as well as changes in the length, argyrophilia, and permeability of the junctions.

Areas of either elongated or "polygonal" cells consistently developed at the same sites in relation to the stenosis, but the hydrodynamic data showed that they did not always correspond (as had been anticipated) to high and low shear, respectively. It is concluded that endothelial cell shape in the living artery must be determined by some other factor(s) in addition to shear stress. (Am J Pathol 1988, 133:407–418)

IT IS WELL established from studies *in vivo*[1–9] and *in vitro*[10–18] that flow conditions affect the morphology and function of endothelial cells. To induce a flow disturbance *in vivo*, a classic method has been to create a stenosis in a large artery by means of a constricting band or ligature.[2–4,7–9] Cell shapes have been studied either *en face*[3–5,8,9,19–21] or indirectly from imprints on a plastic cast.[7,9] One of the basic conclusions has been that elongated cells correspond to regions of increased wall shear stress, while polygonal cells correspond to relatively low shear.

The main goal of this study was to re-examine the correlation between flow conditions and endothelial morphology (including ultrastructure) using the stenosis produced in the aorta of the rat by a U-shaped metal clip applied transversally[6] (Figure 1); the hydrodynamic disturbances were studied in a scaled-up physical model. This type of stenosis has a number of advantages, and it led to the conclusion that the correlation between wall shear stress and endothelial cell shape is not as simple as currently believed.

A second goal was to characterize, by light and electron microscopy, changes of the regenerated endothelium in the throat of the stenosis, where the cells have become adapted to survive a shear stress lethal to normal endothelium.

This paper lays the groundwork for a subsequent study[22] that examines the topography of lipid deposition in hypercholesterolemic rats bearing the "clip-type" stenosis.

Materials and Methods

Animal Model

Overall Experimental Procedure

Eighty-five male Wistar rats weighing 250–300 g were maintained and tested in accordance with recommendations in the *Guide for the Care and Use of Laboratory Animals* and the guidelines of the Animal

Supported in part by Grants HL 25973 and HL 33529 from the National Heart, Lung and Blood Institute.

Accepted for publication July 11, 1988.

Address reprint requests to Thomas Zand, MD, Department of Pathology, University of Massachusetts Medical School, 55 Lake Avenue North, Worcester, MA 01655.

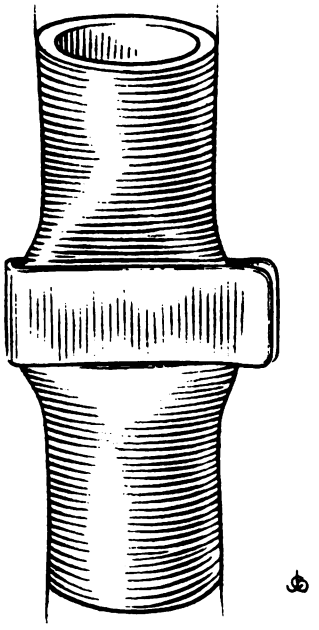

Figure 1—Artist's view of the "transverse clip" stenosing the rat abdominal aorta. Clip width 1 mm; aortic dimensions to scale.

Care Advisory Committee of the University of Massachusetts Medical School. The study focused primarily on the 3-week stage, with additional experiments on either side of this time point (1–7 days, 2–18 months). Animals were killed in 3 groups: 1) permanent stenosis (clip left in place), 2) temporary stenosis controls (clip removed after 1 hour), 3) normal controls (nonclipped). With permanent stenosis at 1–7 days 20 animals were studied, 10 by light microscopy (LM) and 10 by electron microscopy (EM) (one of which received horseradish peroxidase [HRP]). At 3 weeks, 21 animals were studied, 15 by LM (5 by fluorescence), 6 by EM (1 with HRP). At 2–18 months, 9 animals were studied, 2 by LM, 7 by EM (4 with HRP). With temporary stenosis, at 1–7 days 13 animals were examined, 4 by LM, 9 by EM (1 with HRP); at 3 weeks, 5 animals were examined, 2 by LM, 3 by EM (one with HRP); at 2 months, 2 animals were examined by EM with HRP. Ten rats without stenosis, 4 studied by LM, 6 by EM (2 with HRP) were used as normal controls. Five rats with stenosis were used to make casts for the hydrodynamic model.

Surgical procedures were performed as described previously.[6] Stenosis was produced by a U-shaped platinum or silver clip (0.15 mm × 1 mm × 3 mm with a 0.45 mm gap between the arms), which reduced the cross-sectional area of the lumen by 69 ± 5%. In temporary stenosis, when the clip was removed after 1 hour, it was replaced by a thin unrestricting plastic ribbon, so that the experimental area could be identified at time of death.

Processing for Light Microscopy

Aortas used for light microscopy were silver-stained by perfusion.[23] A 5–7 mm segment comprising the stenosis was excised, cut open, laid flat, mounted in Permount, and examined *en face*. Some segments were also stained with hematoxylin before mounting.

Fluorescent Staining

Visualization of F-actin was carried out on clipped aortas using rhodamine-labeled phalloidin (Molecular Probes, Inc., Eugene, OR), with a method modified from White and coworkers[24] and Wong and Gotlieb.[25] With the rat under deep ether anesthesia, the thoracic aorta was cannulated with a 20-gauge Angiocath (Deseret, Sandy, UT) and solutions were infused at 110 mm Hg in the following sequence: 10 mM phosphate-buffered saline (PBS) 1 minute, 3.7% formaldehyde in PBS (pH 7.4) 20 minutes, PBS 2 minutes, 0.1% Triton X-100 (Sigma Chemical Co., St. Louis, MO) in PBS 1 minute and PBS 2 minutes. Segments including the clip site and 1–2 mm either proximal or distal to the clip were then incubated with rhodamine-phalloidin for 20 minutes, at room temperature in a dark, moist atmosphere. The segments were rinsed in PBS, opened, mounted with 10% glycerol, and studied *en face* with epifluorescence optics.

Electron Microscopy

Fixation, embedding, and processing methods have been described.[6] Transverse cuts were made in the middle of the clip area and 1–3 mm above or below the clip. These segments were cut either transversely into rings or longitudinally into strips through the clip area and its immediate proximal or distal edge. Rings 1 mm thick were also cut 3–6 mm proximal and distal to the clip site.

Permeability Tracer

Horseradish peroxidase (HRP) (Type II, Sigma) 10 mg/100 g body weight, was injected intravenously 10 minutes before fixation, and aortic segments were incubated and revealed as described previously.[6]

Morphometry on Light Micrographs

En face preparations of "silvered" aortas from 13 rats (9 with 3-week permanent stenosis and 4 normal controls) were randomly photographed at the throat of the clip site and at its corresponding area between the iliolumbar arteries in controls. Prints were made to an enlargement of ×400 and the number of endothelial cells/sq mm of aortic surface was determined manually. Counts from the micrographs in each

Table 1—Comparison of Aortic Casts and Hydrodynamic Model Dimensions

	Percent stenosis	D (mm)	H (mm)	L (mm)	W (mm)	Θ (degrees)	TL (mm)
Casts (N = 5) Mean ± SD	69 ± 5	1.32 ± 0.21	0.30 ± 0.04	0.97 ± 0.11	1.34 ± 0.08	54 ± 10	2.52 ± 0.50
Model*	69	1.48	0.28	0.96	1.96	59	1.68

* Values derived by dividing the actual model dimensions by 68.

group were pooled and averaged. Statistical significance was determined with the Welch-Aspin *t*-test.

Length and Width of Endothelial Cells

From micrographs of silver stained aortas, 500 endothelial cells from normal controls (4 animals) and 500 from the throat of 3-week clip sites (6 animals) were measured and averaged using an HI PAD digitizing tablet (Houston Instruments, Austin, TX) and a PDP 11/40 computer (Digital Electronic Corp., Maynard, MA). Cell length was determined by measuring the longest axis of the cell, cell width by measuring a line across the center of the cell perpendicular to the long axis.

Morphometry on Electron Micrographs

Each specimen was embedded in Epon so as to provide longitudinal sections of the aorta. Eight blocks of 3-week clip sites from three animals, and eight blocks of the mid-abdominal aorta between ilio-lumbar arteries from four normal controls were cut. The sections were mounted on Formvar-coated slot grids, and photographed consecutively at ×11,000. Endothelial cell thickness was determined by measuring, in millimeters, the distance between the luminal and basal plasma membrane in the center of each micrograph; the final value was expressed in microns. The means were derived from 400 measurements of 114 cells from the clip sites and 400 measurements of 126 cells from control areas. For stress fibers, using 379 micrographs of endothelial cells from the clip site and 398 micrographs of cells from control areas, the presence or absence of stress fibers was noted on each micrograph. The number of micrographs containing stress fibers was counted and expressed as a percentage of the total number of micrographs in each group. The lengths of interendothelial junctions were measured on cross sections of the endothelium, cut perpendicularly to the axis of the aorta in mid-stenosis (two animals with 3 months stenosis) and in the corresponding area of one normal control. All visible junctions (100 from the control and 150 from the clipped rats) were photographed. These were traced on transparent plastic and the tracings were measured and averaged.

Hydrodynamic Model

A 68:1 enlarged model of a segment of the rat aorta, including the stenotic portion, was built using lucite tubing with an inner diameter of 10.1 cm. The dimensions of the rat aorta were obtained from casts prepared from 5 stenotic aortas.[26] The casts were measured using an optical comparator (model PC-14, Jones and Lamson, Springfield, VT). The model was produced by heating the lucite tubing to 95 C, compressing it to the desired shape in a fixture and allowing it to cool. Table 1 compares the dimensions of the actual aortic stenoses with those of the model stenosis. The model provides an accurate representation of four critical dimensions associated with the throat of the stenosis (Figure 2): the percent area reduction, height (H), length (L), and maximum angle of the sloping walls at the entrance and exit of the stenosis (θ). The perimeter of the rat aorta in the stenotic segment shrinks 20%, however, whereas in the model it shrinks by only 5%. Consequently the lateral bulges of the flattened aorta (W in Table 1 and Figure 2) are proportionately smaller than in the model. Also, the length of the segment affected by the clip (TL) is greater in the actual aorta. These two minor discrepancies are due to the elastic properties of the aortic wall.

Steady flow was used for the hydrodynamic measurements in the model for the following reasons. Based on dimensional analysis of the momentum equation, the unsteady acceleration due to pulsatile flow may be neglected in the vicinity of the stenosis if it is much smaller than the acceleration due to the axial variation of the vessel geometry. Quantitatively this occurs when $4\ \alpha^2/\mathrm{Re} \ll 1$ where the Womersley number α is given by $\sqrt{\omega/\nu}\ \mathrm{D}/2$ and the Reynolds number is UD/ν. The diameter (D = 1.3 mm) and the average velocity (U = 0.81 m/s) are for flow in the unobstructed vessel; ($\nu = 3.8 \times 10^{-6}$ sq m/s) is the kinematic viscosity and ($\omega = 31\ \mathrm{s}^{-1}$) is the circular frequency of the heart rate. For the rat aorta $4\ \alpha^2/\mathrm{Re}$ is approximately 0.05, which indicates that the flow in the stenotic region (length TL in Figure 2) may be regarded as quasi-steady. In quasi-steady flow, the velocity profile associated with the instantaneous flow at

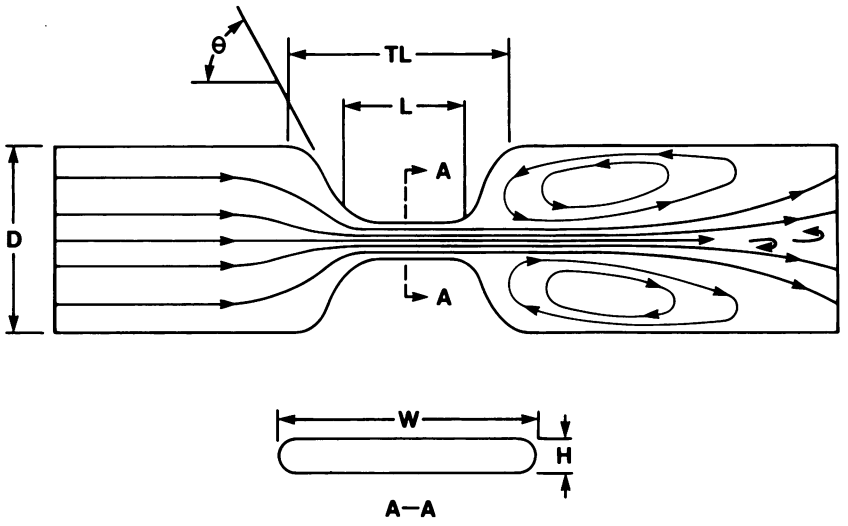

Figure 2—Schematic sagittal view of the hydrodynamic model, showing flow field as observed with neutrally buoyant hydrogen bubbles. Letters correspond to those of Table 1; A-A = cross section through the stenosis.

any time during the pulsatile cycle will be identical to the steady velocity profile at that same flow rate. Outside the stenotic region the flow is not quasi-steady and pulsatile effects have to be considered.

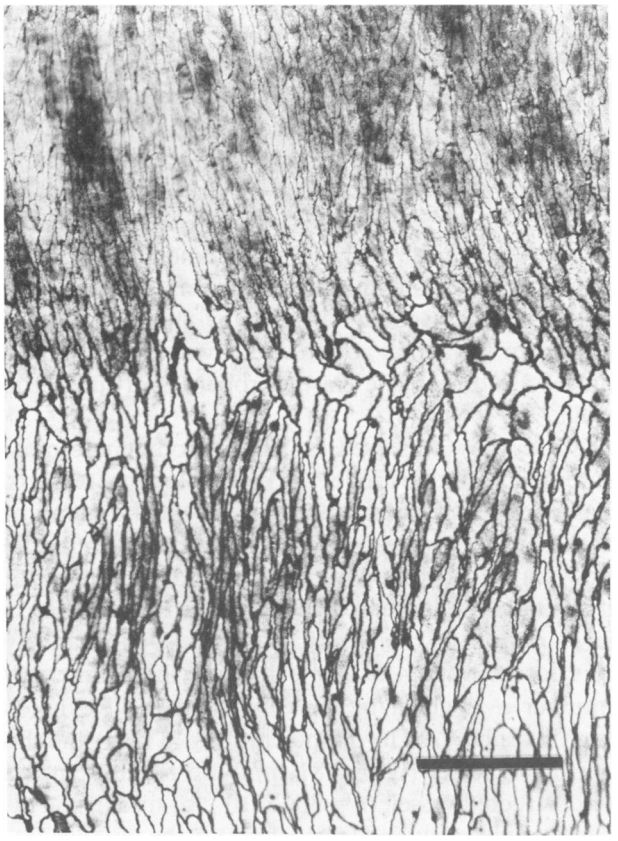

Figure 3—Permanent stenosis, 1 week; *en face* view of clip site (top) and distal aorta. Flow from top to bottom. At the clip site the endothelial cells are thinner, longer and more numerous; darkly stained areas represent subendothelial leukocytes. The distal aorta has a patch of long, thin endothelial cells; between this and the clip site there is a band of wider less axially oriented endothelial cells (polygonal cells). Silver impregnation and hematoxylin; bar = 0.1 mm.

To achieve measurable velocities using enlarged Reynolds number scaled models, air was used as a working fluid. Steady flow studies were performed at unobstructed Reynolds numbers of 230, 340, 450, and 560, which approximate 40, 60, 80, and 100% of peak systolic flow in the rat.[27] Compressed air flowed through a regulator, a rotameter, and into a 3-m long pipe which provided fully developed laminar flow at the stenosis inlet. Downstream of the test section the air entered a 0.2 cu m plenum chamber before dispersal to the atmosphere.

Velocity profiles were measured using a DISA constant temperature anemometer (type 56C01 with a 56C16 bridge) with a tungsten-platinum coated probe using a computer data acquisition system. The probe was calibrated using the rotameter and the fully developed laminar velocity profile (Poiseuille flow) that existed at the exit of the 3-m pipe. A positioning apparatus with a vernier scale allowed the hot wire probe to be moved in 0.1-mm increments, and within 1 mm of the model wall.

To determine the wall shear, additional velocity measurements were made between 1.0 mm and 4.5 mm of the wall surface in 0.5 mm increments. A quadratic curve fitted to each of 5 data sets near the wall and the slope of the velocity profile at the wall was used to calculate the dimensionless shear (τ/τ_0), where τ_0 is the wall shear stress in the unobstructed vessel. While the numerical magnitude of wall shear depends on the Reynolds number, the results will show that the dimensionless shear is not a strong function of the Reynolds number.

Flow Visualization

To determine the direction of flow at points where the hot wire probe velocity measurements were made,

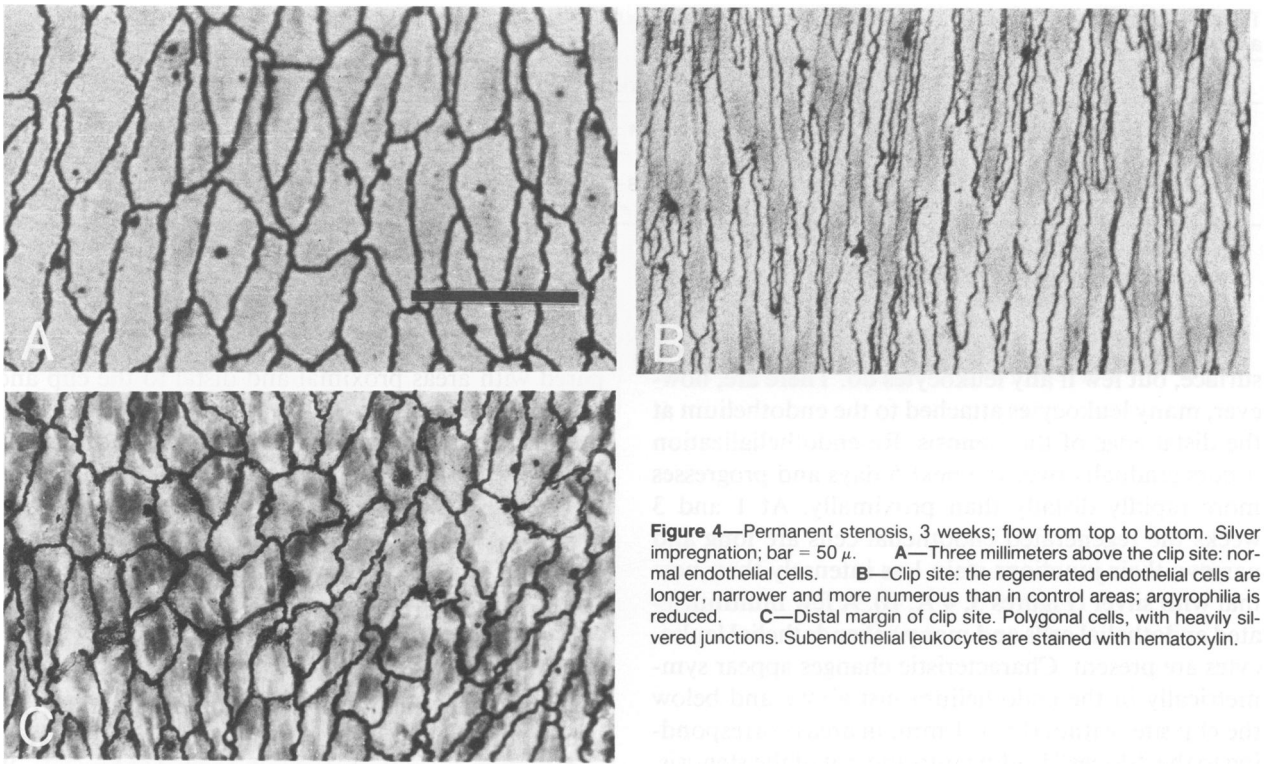

Figure 4—Permanent stenosis, 3 weeks; flow from top to bottom. Silver impregnation; bar = 50 μ. **A**—Three millimeters above the clip site: normal endothelial cells. **B**—Clip site: the regenerated endothelial cells are longer, narrower and more numerous than in control areas; argyrophilia is reduced. **C**—Distal margin of clip site. Polygonal cells, with heavily silvered junctions. Subendothelial leukocytes are stained with hematoxylin.

visualization studies were performed using titanium tetrachloride or neutrally buoyant hydrogen bubbles.

Results

Animal Model

Light Microscopy

Temporary Stenosis

Silver-stained preparations of temporary stenosis controls showed that after 60 minutes of stenosis a band of endothelium was almost completely removed. One day after injury most of the former clip site is partially covered by new endothelium, and by 3 days it is completely covered. By 7 days most of the regenerated endothelial cells are axially oriented, and at 3 weeks the endothelium is indistinguishable from normal areas several millimeters up or downstream.

Permanent Stenosis

At 1 day most of the endothelium is still missing. Streaks and clumps of platelets stick to the denuded

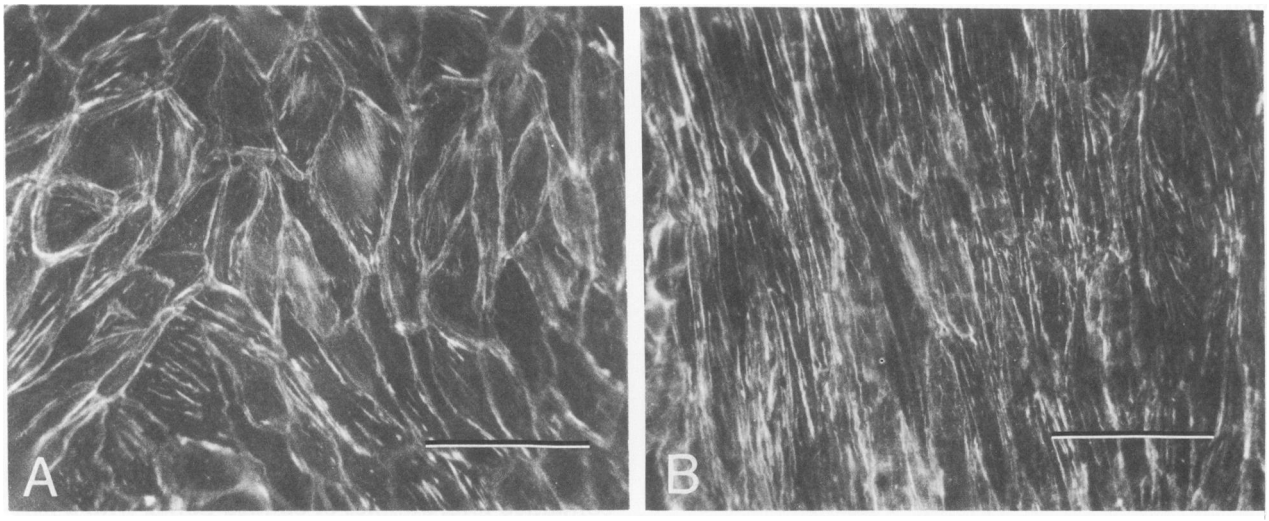

Figure 5—Permanent stenosis, 3 weeks. Flow from top to bottom; rhodamine-labeled phalloidin (UV light, bar = 50 μ). **A**—Control area, 4–5 mm distal to the clip site. Endothelial cells are characterized by a peripheral band of fluorescence and irregularly oriented stress fibers. **B**—Clip site. Stress fibers strictly oriented in the direction of flow; peripheral actin has largely disappeared.

Table 2—Morphometric Comparisons of Control Aortas and 3 Week Clip Sites Regarding Endothelial Cell Dimensions (μ) and the Number of Endothelial Cells/sq mm (Mean ± SEM)

	Length*	Width*	Thickness*	Cells/sq mm†
Control (nonclipped)	68.7 ± 0.8 (N = 500)	13.4 ± 0.2 (N = 500)	0.81 ± 0.02 (N = 400)	1737 ± 64 (N = 14)
3 week clip site	84.5 ± 0.8‡ (N = 500)	8.8 ± 0.1‡ (N = 500)	1.39 ± 0.03‡ (N = 400)	2773 ± 116‡ (N = 21)

* N = number of measurements.
† N = number of light micrographs counted.
‡ $P < 0.00001$, Welch-Aspin t-test.

surface, but few if any leukocytes do. There are, however, many leukocytes attached to the endothelium at the distal edge of the stenosis. Re-endothelialization occurs gradually over the next 5 days and progresses more rapidly distally than proximally. At 1 and 3 weeks the regenerated endothelial cells are long and narrow; their junctions stain less intensely than normal with silver (Figures 3, 4 A, B). A few multinucleated endothelial cells and many subendothelial leukocytes are present. Characteristic changes appear symmetrically in the endothelium just above and below the clip site, within 0.5 to 1 mm, in areas corresponding to the "slopes" leading into and out of the stenosis. Along the edges of the clip site are two transverse bands of polygonal cells, shorter, wider, and with more argyrophilic junctions (Figure 4C). These bands are 2–5 cells wide. Farther away from the clip site (proximally and distally) is a patch of elongated cells, also with heavily silver-stained junctions; both the proximal and the distal patches are roughly triangular, with a base toward the polygonal cells and the apex pointing away from the clip site (Figure 3).

Rats given injections of HRP showed that the endothelium in the area of stenosis (although apparently well regenerated) was abnormally permeable, as compared with areas proximal and distal to the clip and with normal controls. This was obvious at 3 weeks, 3 months, and to a lesser degree even at 18 months.

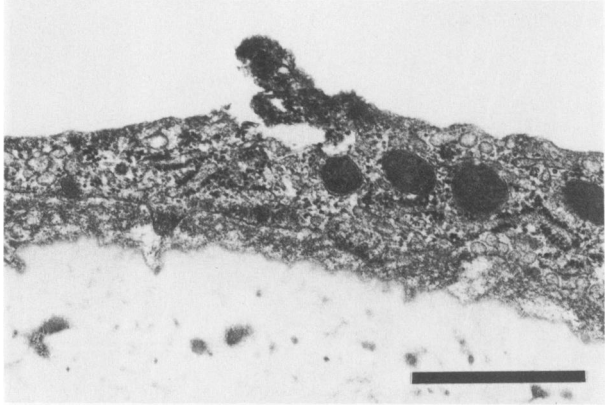

Figure 6—Permanent stenosis, 6 days. Clip area. Partial injury of a regenerated endothelial cell: focal membrane disruption and cytoplasmic osmiophilia (micro-ulcer). Bar = 1 μ.

Localization of F-actin

In areas 3–6 mm proximal or distal to the clip site, where endothelial patterns were the same as in controls, all cells were characterized by a peripheral (cortical) band of fluorescence. The overall appearance recalled the pattern of "silver lines." Intracellular stress fibers (straight filaments of actin-positive material) were extremely variable in length, thickness, and orientation: wider endothelial cells tended to have small, thick stress fibers, not always aligned along the axis of the aorta, or large bundles of very thin stress fibers; longer cells tended to have longer stress fibers oriented along the cell's main axis. Both cell types could be seen juxtaposed in the same microscopic field (Figure 5A). At the clip site the cortical band of actin was virtually absent, thus the cellular outline was not recognizable. Stress fibers were strictly oriented in the direction of flow, and more tightly packed; they could be short or long, and often appeared thicker than normal (Figure 5B).

Morphometric Data on Light Micrographs

In the throat of the stenosis, after 3 weeks, the cells had become 23% longer, 34% narrower, and 60% more numerous (Table 2).

Electron Microscopy

In temporary stenosis controls the process of endothelial regeneration was essentially the same as reported by others after endothelial denudation.[28–30] In permanent stenosis Weibel-Palade bodies were present in the new endothelial cells as early as day 3; during the first week the new endothelial cells showed occasional signs of surface injury, ie, micro-ulcers[6] (Figure 6). Already during this stage regenerating cells contained long bundles of banded fibrils, with a periodicity of 550–650 nm, oriented with the long axis of the cell (stress fibers). Often these fibers ran just be-

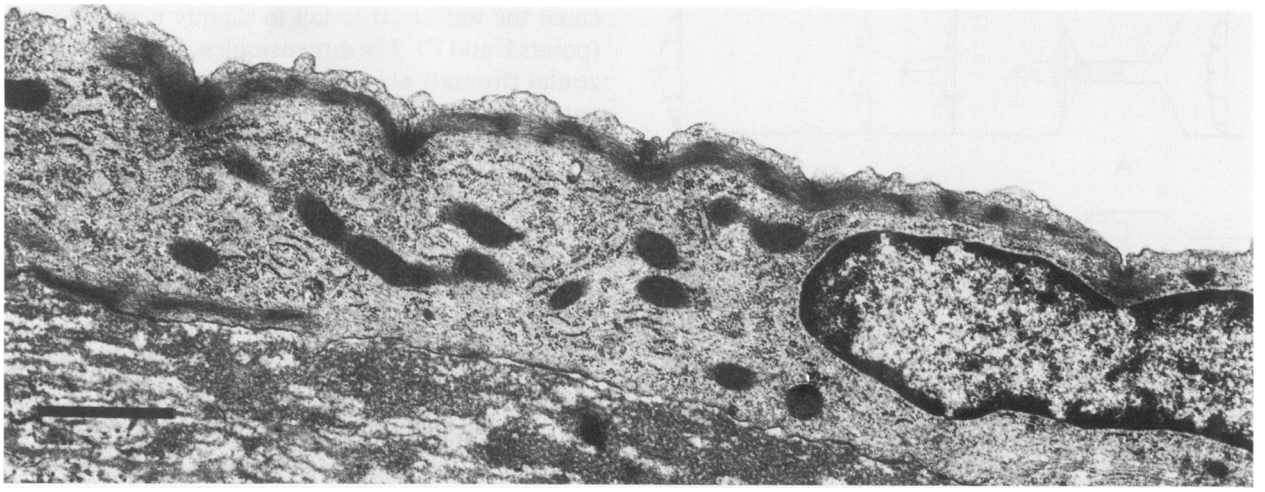

Figure 7—Permanent stenosis, 3 weeks. Clip area. Note bundle of fibrils running just beneath the luminal plasma membrane of the endothelial cell. Bar = 1 μ.

neath the luminal plasma membrane of the cell, where they were never found in controls (Figure 7). Others ran along the abluminal surface and/or criss-crossed the cytoplasm. Many were inserted onto the basal surface of the cell, and appeared to be continuous with a bundle of extracellular fibrils (Figure 8).

Morphometric data from electron micrographs showed at 3 weeks (at which time the endothelium appears stabilized) a 72% increase in the thickness of the endothelial cells (Table 2). Stress fibers were seen in 11% (44 of 398) of the micrographs of control endothelial cells and in 37% (139 of 379) of the micrographs of endothelial cells from clip sites ($P < 0.00001$). The length of the interendothelial junctions at three months of stenosis (1.7 ± 0.09 μ) showed a 32% decrease ($P < 0.00001$) as compared with controls (2.5 ± 0.11 μ).

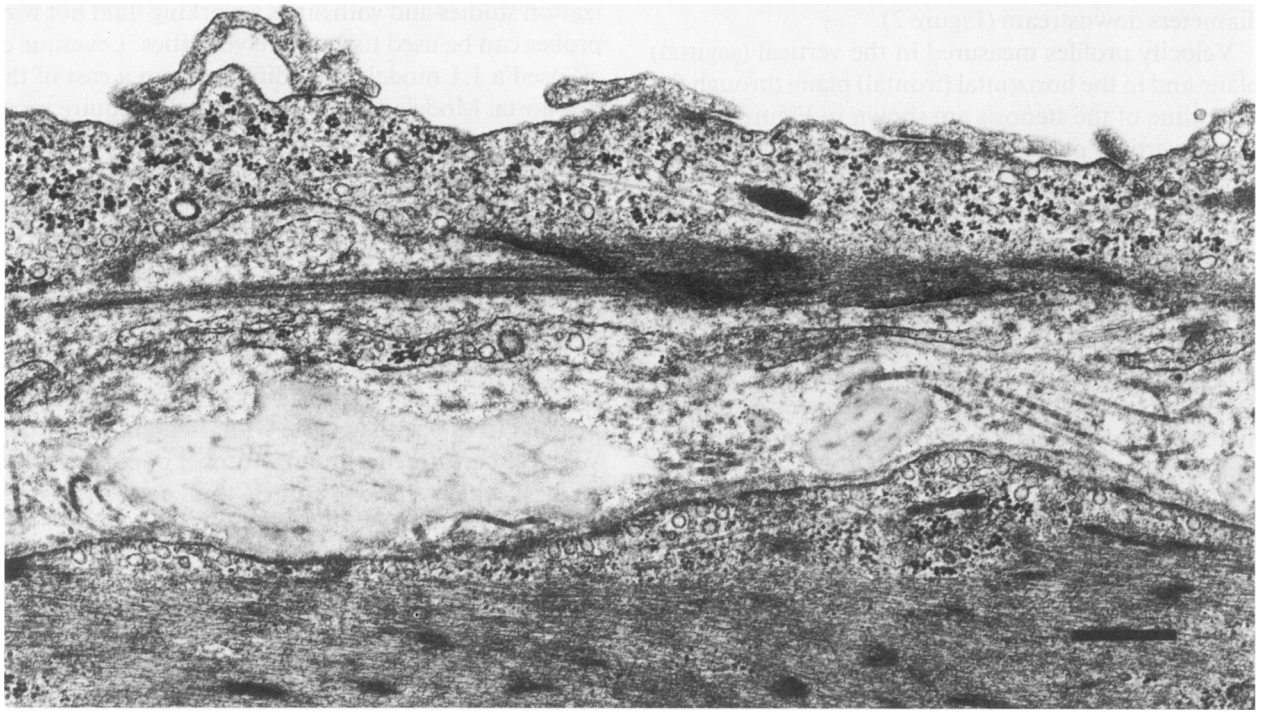

Figure 8—Permanent stenosis, 3 weeks. Clip area. Bundles of fibrils inserted onto the basal surface of the endothelial cells are continuous with bundles of extracellular fibrils (microtendons) Bar = 0.5 μ.

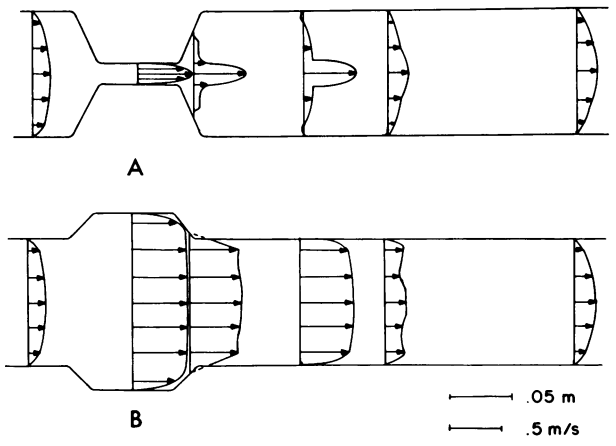

Figure 9—Velocities (m/s) measured in a 68:1 scale model of a 69% stenosis at Re = 560. **A**—Velocity profiles in the vertical plane. Velocities in the rat aorta are 12.9 times the velocities in the model. **B**—Velocity profiles in a horizontal plane passing through the centerline.

Hydrodynamic Model

Flow visualization studies revealed that the entire throat of the stenosis was marked by fast moving laminar flow. Near-stagnation conditions occurred in a small region at the beginning of the steeply sloping wall in the converging inlet section of the stenosis and in a region extending for about one tube diameter downstream. Separated and reverse flow were also present in the downstream region. A small spiral vortex traveled down the center of the tube from 1 diameter after the stenosis to the exit of the test section 3 diameters downstream (Figure 2).

Velocity profiles measured in the vertical (sagittal) plane and in the horizontal (frontal) plane through the centerline of the stenosis are shown in Figure 9 A, B. In the vertical plane, regions of slow flow exist near the wall at the beginning of the converging section. The fluid then accelerates throughout the converging section. In the horizontal plane the velocity profiles are reasonably flat. In the throat of the stenosis both the vertical and horizontal plane profiles show fast moving laminar flow. At the exit of the stenosis, the vertical profile shows severe jetting with flow reversal occurring for almost one diameter downstream. By 2 diameters downstream, both velocity profiles are reasonably flat.

The dimensionless shear is only weakly dependent upon the Reynolds number (Figure 10 B, C). In the vertical (sagittal) plane (Figure 10B) the wall shear stress falls as the flow first enters the converging approach to the stenosis (point A) and then rises rapidly to approximately 25 times the upstream value (points C and D). The dimensionless shear then falls to about 15 times as the flow proceeds through the stenosis throat. At the throat exit separated and reverse flow cause the wall shear to fall to slightly negative values (points E and F). The dimensionless shear, in the horizontal (frontal) plane (Figure 10C), rises as the flow enters the bulge of the stenosis to 10 times the upstream value (point G) and remains elevated in the region downstream of the stenosis (point H).

Discussion

Critique of the Models

Anatomically, the "transverse clip" stenosis is advantageous because the degree of stenosis is easily controllable, and the intima in the throat of the stenosis remains flat. When constricting rings or bands are used to produce a substantial stenosis[2-4,7-9] the intima may form longitudinal folds[7,31] that complicate the interpretation of the changes and may induce endothelial damage.[31] From a hydrodynamic point of view, the transverse "clip" stenosis produces primarily a planar flow with little variation in velocity profile in the horizontal plane except immediately adjacent to the walls. The two-dimensional nature of the flow through the throat makes it easier to model mathematically,[32] and makes the variation in stenosis width between the rat aorta and physical scale model less important.

For the aorta of the rat, the pulsatile flow effect can be neglected in the immediate region of the stenosis. An enlarged, steady flow model enhances flow visualization studies and with air as a working fluid hot wire probes can be used to measure velocities. Levesque et al[9] used a 1:1 model made directly from a cast of the dog aorta. Models of such size generally require more complex velocity measurement techniques such as laser doppler anemometry (LDA). Enlarged scale models are required in our work since even LDA measurements would not suffice in a 1:1 model of the rat aorta.

Shear stress values in the stenosis can be predicted with reasonable certainty because the flow studies were performed using a correctly scaled model. The range of Reynolds numbers corresponds to different instants in the cardiac cycle with different flow rates. We have performed a limited number of pulsatile flow studies which have verified this correspondence within the stenosis.[33]

Effect of Stenosis on Endothelial Regeneration

The time required by new endothelium to cover the denuded area was 3 days in control rats with temporary stenosis, the same as reported for an endothelial denudation of similar width.[30] With permanent steno-

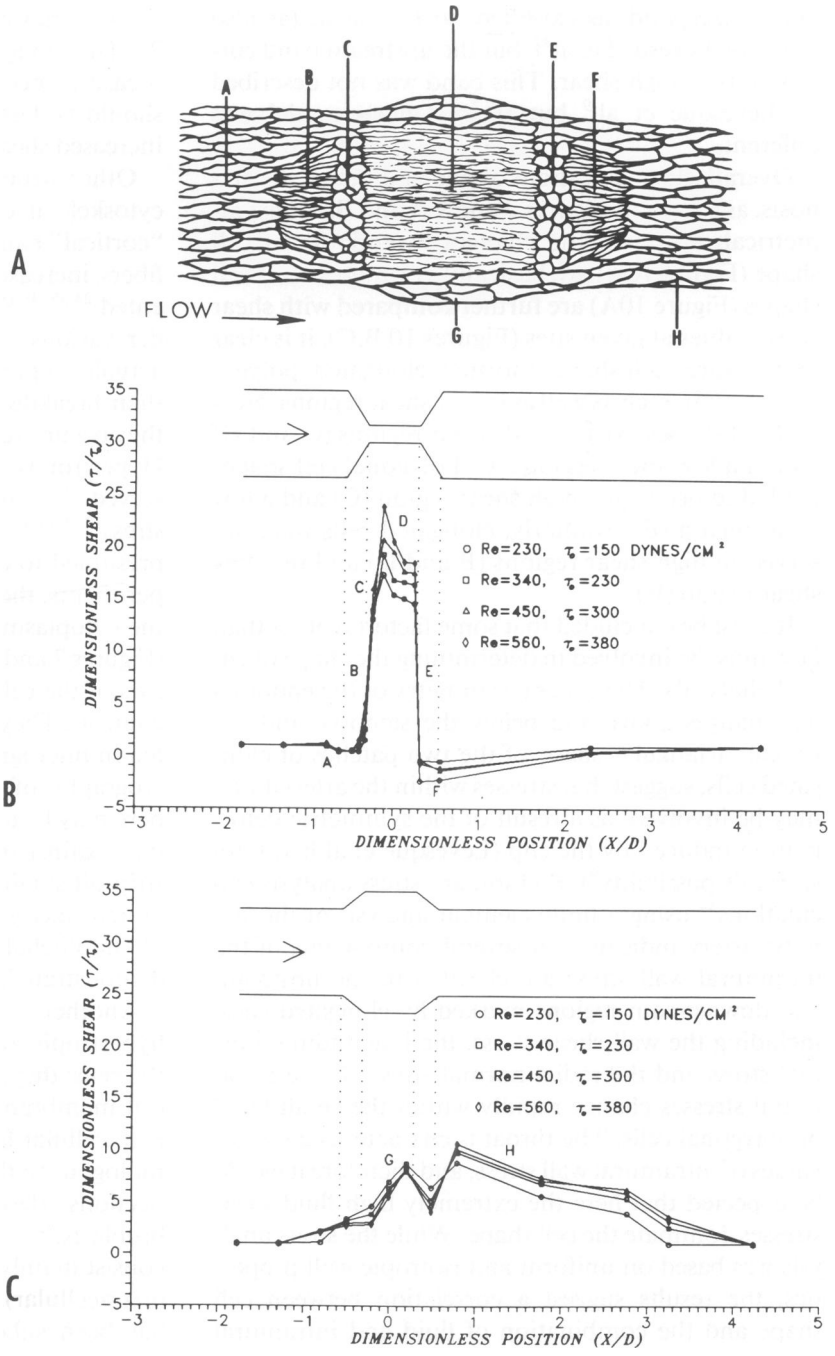

Figure 10—Correlation between endothelial cell shape and wall shear stress. **A**—Scheme of endothelial cell shapes in the stenosis and adjacent aortic intima viewed *en face*. **B**—Dimensionless wall shear stress (τ/τ_0) in the vertical plane. **C**—The horizontal plane. Letters refer to comparable sites in the artery and in the model. X is the axial position measured from the center of the stenosis, D is the vessel diameter.

sis it was more than doubled, to 7 days. This could reflect a repeated loss of regenerating cells due to the continuously elevated shear stress, a slower growth of the cells, or both. Langille and coworkers[8] found that in rabbits high shear retards healing, whereas low shear can enhance it.

Correlation Between Endothelial Cell Shape and Wall Shear Stress

It had been anticipated that elongated cells would consistently correspond to areas of high wall shear stress, and polygonal cells to areas of low shear, as shown by many studies *in vivo*[4,5,7–9,19,21] and *in vitro*,[13–15,18] but such a simple correlation is not apparent in this model. The expected correlation was found in the throat of the stenosis, where the hydrodynamic model indicated a shear stress up to 25 times normal (in absolute terms, of the order of 6–10,000 dynes/sq cm); here the endothelial cells were significantly elongated (Figures 3 and 4B). This area is limited by two bands of polygonal cells: endothelial cells of this shape have been called hexagonal.[20] The downstream band

does correspond, as expected, to low shear (as also noted by Levesque et al[9]), but the upstream band corresponds to high shear. This band was not described by Levesque et al,[9] but their stenosis model was different.

Overall, flow conditions above and below the stenosis, as shown in Figures 2 and 9 A and B, are asymmetrical; however, the changes in endothelial cell shape (Figure 10A) are basically symmetrical. If cell shapes (Figure 10A) are further compared with shear stress values at given sites (Figures 10 B,C), it is clear that all three cell shapes (normal, elongated, polygonal) occur in high as well as in low shear regions. Normal cell shapes exist in high shear regions (G and H) and in a low shear region (A). Polygonal cell shapes tended to occur in a high shear region (C) and a low shear region (E). Similarly, elongated cells were observed in high shear regions (B and D) and in a low shear region (F).

It must be concluded that some factor(s) other than flow must be involved in determining the shape of endothelial cells. The general symmetry of the endothelial changes above and below the stenosis, and the roughly triangular shape of the two patches of elongated cells, suggest that stresses within the arterial wall may be involved, as a result of the symmetric deformation induced by the clip (Levesque et al had foreseen this possibility[9]). Preliminary stress analysis calculations[34] using a finite-element analysis of the stenotic artery indicate that several components of the intramural wall stress are elevated in the upstream and downstream regions marked by elongated cells, including the wall shear stress, the longitudinal normal stress and the radial normal stress. These intramural stresses change rapidly within the small band of polygonal cells. The throat is characterized by low values of intramural wall stress, and therefore it would be expected that here the extremely high fluid shear stresses dominate the cell shape. While the stress analysis was based on uniform and isotropic wall properties, the results suggest a correlation between cell shape and the combination of fluid and intramural wall shear stress.

Endothelial Adaptations in the Zone of Highest Shear

In the throat of the stenosis, the shear stress was sufficient to wipe away the normal endothelium. The regenerated endothelium had therefore become adapted to survive under the new, more demanding conditions. Signs of adaptation were found at the light microscopic and ultrastructural level. The endothelial cells became 23% longer, 34% narrower, and 72% thicker; they also increased in number by 60% (Table 2). The elongation can be seen as a useful adaptive measure, because longitudinally-oriented junctions should be less susceptible to being torn open by the increased shearing force.

Other structural expressions of adaptation are the cytoskeletal changes (Figures 5 A, B): the normal "cortical" band of F-actin fades away, while the stress fibers increase in number, and become axially oriented.[24,35–38] Similar changes have been observed under various experimental conditions[36,37,39] and may actually represent intracellular redistribution rather than breakdown and resynthesis of F-actin, because they occur even after inhibition of protein synthesis.[37] Hypertrophy of the stress fiber system has been observed in endothelial cultures exposed to shear stress[12,16,17,40] as well as *in situ* in the rat aorta, in areas presumed to correspond to high shear.[24] In these experiments, the stress fibers could be seen anywhere in the cytoplasm, and also beneath the luminal surface (Figures 7 and 8) where they are oriented with the long axis of the cell. They are not seen in this location in controls. They were seen more than three times as often in micrographs of adapted endothelium as in micrographs of control endothelium. Their function here may be to stiffen the surface of the cell as protection against the increased shearing force, which can strip off small portions of the cell surface and create "micro-ulcers" (Figure 6). An increase in the rigidity of endothelial cells submitted to high shear has been demonstrated.[14]

Another endothelial adaptation to high shear is the hypertrophy of the anchoring structures at the base of the cells; they consist of stress fibers inserted onto the cell membrane, and are apparently continuous with extracellular fibrillar bundles. They are probably homologous to the cell-to-substrate and cell-to-cell connections described for fibroblasts[41] and myofibroblasts;[42,43] these have been named fibronexus and consist mainly of actin (intracellular) and fibronectin (extracellular). The arrangement shown in Figure 8 has been subclassified as tandem fibronexus;[42] the term *microtendon*[44] seems more evocative.

In conclusion, this study has shown that 1) endothelial cell shape is determined not only by fluid shear stress but also by other factors, most likely stresses within the arterial wall; 2) endothelium regenerating under high shear grows more slowly but modulates into a cell type (adapted endothelium) that can survive a shear stress of up to 10,000 dynes/sq cm lethal to normal endothelium; and 3) this adaptation includes changes in cell orientation, number, length, width, thickness, stress fibers, and anchoring structures, as well as changes in the length, argyrophilia and

permeability of the intercellular junctions. These changes should be pertinent to the endothelium of arteries made stenotic by atherosclerotic plaques.

References

1. Fry DL: Acute vascular endothelial changes associated with increased blood velocity gradients. Circ Res 1968, 22:165–197
2. Glagov S, Ts'ao Chung-hsin: Restitution of aortic wall after sustained necrotizing transmural ligation injury. Am J Pathol 1975, 79:7–30
3. Gerrity RG, Naito HK: Alteration of endothelial cell surface morphology after experimental aortic coarctation. Artery 1980, 8:267–274
4. Reidy MA, Langille BL: The effect of local blood flow patterns on endothelial cell morphology. Exp Molec Pathol 1980, 32:276–289
5. Greenhill NS, Stehbens WE: Scanning electron microscopic study of the anastomosed vein of arteriovenous fistulae. Atherosclerosis 1981, 39:383–393
6. Joris I, Zand T, Majno G: Hydrodynamic injury of the endothelium in acute aortic stenosis. Am J Pathol 1982, 106:394–408
7. Legg MJ, Gow BS: Scanning electron microscopy of endothelium around an experimental stenosis in the rabbit aorta using a new casting material. Atherosclerosis 1982, 42:299–318
8. Langille BL, Reidy MA, Kline RL: Injury and repair of endothelium at sites of flow disturbances near abdominal aortic coarctations in rabbits. Arteriosclerosis 1986, 6:146–154
9. Levesque MJ, Liepsch D, Moravec S, Nerem RM: Correlation of endothelial cell shape and wall shear stress in a stenosed dog aorta. Arteriosclerosis 1986, 6:220–229
10. Dewey CF Jr, Bussolari SR, Gimbrone MA Jr, Davies PF: The dynamic response of vascular endothelial cells to fluid shear stress. J Biomech Eng 1981, 103:177–185
11. White GE, Fujiwara K, Shefton EJ, Dewey CF, Gimbrone MA Jr: Fluid shear stress influences cell shape and cytoskeleton organization in cultured vascular endothelium. Fed Proc 1982, 41:321
12. Franke R-P, Gräfe M, Schnittler H, Seiffge D, Mittermayer C, Drenckhahn D: Induction of human vascular endothelial stress fibers by fluid shear stress. Nature 1984, 307:648–649
13. Eskin SG, Ives CL, McIntire LV, Navarro LT: Response of cultured endothelial cells to steady flow. Microvasc Res 1984, 28:87–94
14. Nerem RM, Sato M, Levesque MJ: Elongation orientation and effective shear modulus of cultured endothelial cells in response to shear. Fed Proc 1985, 44:1659
15. Levesque MJ, Nerem RM: The elongation and orientation of cultured endothelial cells in response to shear stress. J Biomech Eng 1985, 107:341–347
16. Wechezak AR, Viggers RF, Sauvage LR: Fibronectin and F-actin redistribution in cultured endothelial cells exposed to shear stress. Lab Invest 1985, 53:639–647
17. Ives CL, Eskin SG, McIntire LV: Mechanical effects on endothelial cell morphology: In vitro assessment. In Vitro Cell Develop Biol 1986, 22:500–507
18. Viggers RF, Wechezak AR, Sauvage LR: An apparatus to study the response of cultured endothelium to shear stress. J Biomech Eng 1986, 108:332–337
19. Silkworth JB, Stehbens WE: The shape of endothelial cells in en face preparations of rabbit blood vessels. Angiol 1975, 26:474–487
20. Collatz Christensen B, Chemnitz J, Tkocz I, Blaabjerg O: Repair in arterial tissue. The role of endothelium in the permeability of a healing intimal surface: Vital staining with Evans blue and silver staining of the aortic intima after a single dilatation trauma. Acta Path Microbiol Scan Sect A 1977, 85:297–310
21. Kibria G, Heath D, Smith P, Biggar R: Pulmonary endothelial pavement patterns. Thorax 1980, 35:186–191
22. Zand T, Majno G, Nunnari JJ, Hoffman AH, Savilonis BJ, MacWilliams B, Joris I: Correlation between shear stress and intimal lipid deposition: A study in hypercholesterolemic rats with aortic stenosis. Submitted for publication
23. Zand T, Underwood JM, Nunnari JJ, Majno G, Joris I: Endothelium and "silver lines": An electron microscopic study. Virchows Arch [A] 1982, 395:133–144
24. White GE, Gimbrone MA Jr, Fujiwara K: Factors influencing the expression of stress fibers in vascular endothelial cells in situ. J Cell Biol 1983, 97:416–424
25. Wong MKK, Gotlieb AI: *In vitro* reendothelialization of a single-cell wound: Role of microfilament bundles in rapid lamellipodia-mediated wound closure. Lab Invest 1984, 51:75–81
26. Levesque MJ, Cornhill FJ, Nerem RM: Vascular casting. A new method for the study of arterial endothelium. Atherosclerosis 1979, 34:457–467
27. Altman PL, Dittmer DS: Biology Data Book. Vol. 3, 2nd ed. Bethesda, FASEB, 1974, p 1741
28. Haudenschild CC, Schwartz SM: Endothelial regeneration. II. Restitution of endothelial continuity. Lab Invest 1979, 41:407–418
29. Reidy MA, Schwartz SM: Endothelial regeneration. Time course of intimal changes after small defined injury to rat aortic endothelium. Lab Invest 1981, 44:301–308
30. Reidy MA, Silver M: Endothelial regeneration. VII. Lack of intimal proliferation after defined injury to rat aorta. Am J Pathol 1985, 118:173–177
31. Joris I, Majno G: Endothelial changes induced by arterial spasm. Am J Pathol 1981, 102:346–358
32. Savilonis BJ, Hoffman AH, LaCoy DR Jr, Soebroto SP, Holzman JJ Jr: Using hydrodynamic scale models and computer simulations to study the flow thru a transverse clip stenosis, Advances in Bioengineering. New York, ASME, 1984, pp 115–116
33. Savilonis BJ, Hoffman AH, Berg PL, Fedele BB, Pacecca RA: Experimental studies of pulsatile flow thru a transverse clip stenosis, Proceedings of the Twelfth Northeast Bioengineering Conference. Edited by SC Orphanoudakis. New York, IEEE, 1986, pp. 277–280
34. MacWilliams BA, Savilonis BJ, Hoffman AH: Modeling lipid transport through the transverse clip stenosis, Proceedings of the Fourteenth Northeast Bioengineering Conference. New York, IEEE, 1988, in press
35. Herman IM, Pollard TD, Wong AT: Contractile proteins in endothelial cells. Ann NY Acad Sci 1982, 401:50–60
36. Gabbiani G, Gabbiani F, Lombardi D, Schwartz SM: Organization of actin cytoskeleton in normal and regenerating arterial endothelial cells. Proc Natl Acad Sci USA 1983, 80:2361–2364
37. Byers HR, White GE, Fujiwara K: Organization and function of stress fibers in cells in vitro and in situ: A

review, Cell and muscle motility, Vol. 5, The Cytoskeleton. Edited by JW Shay. New York, Plenum Press, 1984, pp 83–137
38. Hüttner I, Walker C, Gabbiani G: Aortic endothelial cell during regeneration: Remodeling of cell junctions, stress fibers, and stress fiber-membrane attachment domains. Lab Invest 1985, 53:287–302
39. Gotlieb AI, Spector W, Wong MKK, Lacey C: In vitro reendothelialization: Microfilament bundle reorganization in migrating porcine endothelial cells. Arteriosclerosis 1984, 4:91–96
40. Dewey CF Jr: Effects of fluid flow on living vascular cells. J Biomech Eng 1984, 106:31–35
41. Chen W-T, Singer SJ: Immunoelectron microscopic studies of the sites of cell-substratum and cell-cell contacts in cultured fibroblasts. J Cell Biol 1982, 95:205–222
42. Singer II, Kawka DW, Kazazis DM, Clark RAF: In vivo codistribution of fibronectin and actin fibers in granulation tissue: Immunofluorescence and electron microscope studies of the fibronexus at the myofibroblast surface. J Cell Biol 1984, 98:2091–2106
43. Singer II, Kazazis DM, Kawka DW: Localization of the fibronexus at the surface of granulation tissue myofibroblasts using double-label immunogold electron microscopy on ultrathin frozen sections. Eur J Cell Biol 1985, 38:94–101
44. Ryan GB, Cliff WJ, Gabbiani G, Irlé C, Montandon D, Statkov PR, Majno G: Myofibroblasts in human granulation tissue. Hum Pathol 1974, 5:55–67

Acknowledgment

The authors thank Christopher D. Hebert for the photographic prints, and Jane M. Manzi and Linda M. Johnston for the preparation of the manuscript.